REPORT DOCUMENTATION PAGE

Form Approved
OMB No. 0704-0188

1. REPORT DATE *(DD-MM-YYYY)*	2. REPORT TYPE	3. DATES COVERED *(From - To)*
03-06-2008	Technical Paper	

4. TITLE AND SUBTITLE

Development of a Prototype Rocket Engine for a Nanosat Launch Vehicle First Stage (Preprint)

5a. CONTRACT NUMBER
FA9300-06-C-0009

5b. GRANT NUMBER

5c. PROGRAM ELEMENT NUMBER

6. AUTHOR(S)
George Haberstroh & Eric Besnard (CSULB); Matthew Baker & John Gavey (Garvey Spacecraft Corporation)

5d. PROJECT NUMBER

5e. TASK NUMBER

5f. WORK UNIT NUMBER
300506F9

7. PERFORMING ORGANIZATION NAME(S) AND ADDRESS(ES)

Garvey Spacecraft Corporation
389 Haines Avenue
Long Beach CA 90814-1841

8. PERFORMING ORGANIZATION REPORT NUMBER

AFRL-RZ-ED-TP-2008-195

9. SPONSORING / MONITORING AGENCY NAME(S) AND ADDRESS(ES)

Air Force Research Laboratory (AFMC)
AFRL/RZS
5 Pollux Drive
Edwards AFB CA 93524-7048

10. SPONSOR/MONITOR'S ACRONYM(S)

11. SPONSOR/MONITOR'S NUMBER(S)
AFRL-RZ-ED-TP-2008-195

12. DISTRIBUTION / AVAILABILITY STATEMENT

Approved for public release; distribution unlimited (PA #08232A).

13. SUPPLEMENTARY NOTES
For presentation at the 44th AIAA Joint Propulsion Conference, Hartford, CT, 20-23 July 2008.

14. ABSTRACT

The paper discusses the development of a 4,500 lbf thrust liquid oxygen (LOX)/ethanol rocket engine designed to power a family of suborbital Reusable Nanosat Launch Vehicles (RNLV). In order to meet the range of missions required under the project, the engine is designed to be able to operate over a large performance envelope corresponding to thrust level from 3,000 lbf to 5,000 lbf. Propellants are Introduced and mixed in the combustion chamber utilizing a combination of triplet and unlike doublet injector elements. In addition, film cooling is provided in order to extend the life of the ablative chamber. Ignition is accomplished with solid propellant ports mounted on the side of the chamber. Ten (10) static fire tests have been completed to validate the design and to characterize the engine's performance. Initial testing was conducted to validate the ignition algorithm and verify the engine basic integrity at startup. Further testing was conducted to verify engine performance before flight testing. Data shows that the engine can operate at thrust levels between 2500 and 5074 lbf. This successful engine development serves as a precursor to a future NLV first stage engine which will utilize LOX-propylene for added performance.

15. SUBJECT TERMS

16. SECURITY CLASSIFICATION OF:			17. LIMITATION OF ABSTRACT	18. NUMBER OF PAGES	19a. NAME OF RESPONSIBLE PERSON
					Mr. Nils Sedano
a. REPORT	b. ABSTRACT	c. THIS PAGE	SAR	17	19b. TELEPHONE NUMBER *(include area code)*
Unclassified	**Unclassified**	**Unclassified**			N/A

Standard Form 298 (Rev. 8-98)
Prescribed by ANSI Std. 239.18

Development of a Prototype Rocket Engine for a Nanosat Launch Vehicle First Stage (Preprint)

George Haberstroh[1] *and Eric Besnard*[2]

California State University, Long Beach
Long Beach, CA

Matthew Baker[1] *and John Garvey*[3]

Garvey Spacecraft Corporation
Long Beach, CA

The paper discusses the development of a 4,500 lbf thrust liquid oxygen (LOX)/ethanol rocket engine designed to power a family of suborbital Reusable Nanosat Launch Vehicles (RNLV). In order to meet the range of missions required under the project, the engine is designed to be able to operate over a large performance envelope corresponding to thrust level from 3,000 lbf to 5,000 lbf. Propellants are introduced and mixed in the combustion chamber utilizing a combination of triplet and unlike doublet injector elements. In addition, film cooling is provided in order to extend the life of the ablative chamber. Ignition is accomplished with solid propellant ports mounted on the side of the chamber. Ten (10) static fire tests have been completed to validate the design and to characterize the engine's performance. Initial testing was conducted to validate the ignition algorithm and verify the engine basic integrity at startup. Further testing was conducted to verify engine performance before flight testing. Data shows that the engine can operate at thrust levels between 2500 and 5074 lbf. This successful engine development serves as a precursor to a future NLV first stage engine which will utilize LOX-propylene for added performance.

Nomenclature

AFRL	Air Force Research Lab
CSULB	California State University, Long Beach
c*	characteristic velocity
C_F	thrust coefficient
GN_2	gaseous nitrogen
GSC	Garvey Spacecraft Corporation
ISP	specific impulse
LEO	LEO Earth Orbit
LOX	liquid oxygen
NLV	Nanosat Launch Vehicle
O/F	oxidizer to fuel ratio
P	Prospector
RLV	reusable launch vehicle
SFT	static fire test
VSFT	vertical static fire test

---

[1] AIAA Student Member
[2] Professor and AIAA Senior Member
[3] AIAA Senior Member

I. Introduction

The initial Nanosat Launch Vehicle (NLV) concept was first proposed by Garvey Spacecraft Corporation (GSC) and California State University, Long Beach (CSULB) in 2003 using LOX/ethanol as propellants[1]. The configuration underwent a series of trade studies resulting in a 2-stage pressure-fed LOX-densified propylene vehicle, shown in Figure 1[2,3,4], capable of placing a 10 kg (22 lbm) payload into a nominal 250-km altitude polar orbit. The chamber pressure is nominally 2 MPa (300 psi) for the first stage and 1 MPa (150 psi) for the upper stage. Other vehicle characteristics are listed in Table 1. Some of the technological characteristics of the NLV are: composite propellant tanks, densified propylene as fuel[5], hot gaseous helium as pressurant, as well the use of carbon/silicon carbide (C/SiC) or silicon carbide/silicon carbide ceramic matrix composite (SiC/SiC) for the upper stage engine[6].

NLV development continued with the Prospector 5 (P-5) representing the first NLV development hardware, with the design, integration and flight testing of a low fidelity but full scale first stage using an existing 1200 lbf thrust engine.[7,8] The next evolution, P-6, represented the entire full scale NLV with a first stage, still powered by the same 1200 lbf engine, and a simulated second stage. The flight test demonstrated a low altitude in-flight stage separation and recovery of the first stage and simulated second stage.[9] Following these successful flight tests and vehicle recovery, a greater focus was placed on vehicle reusability, with the development and flight test operations of the P-7 vehicle, powered by the same 1,200 lbf thrust engine. The P-7 flew a total of four times, two of which were on the same day (P-7A and -B)[10]. An evolutionary succession is the Prospector-9 which features a pair of large integral composite tanks instead of the cluster of small 2.85 US Gal tanks used in all earlier vehicles and a 4500 lbf engine that is representative of the NLV first stage engine. Figure 2 illustrates the differences between the suborbital P-7 and P-9A/B, and the orbit-capable NLV while Table 2 compares performance values between the aforementioned vehicles. The P-9A/B performance reported in the table corresponds to only 13% of the propellant load in order to keep the vehicle within the test range. Also, to limit lift-off thrust-to-weight ratio, the engine operates at reduced thrust. The fin-stabilized P-9 vehicle, even with only half propellant load, is capable of reaching altitudes in excess of 40 km. With a full load and thrust vector control, its performance will approach that of the operational NLV first stage.

Table 3 compares the nominal engine characteristics and requirements of the first stage engine for both the new family of RNLV vehicles and NLV. The requirements cover a wide range because the engine is to power not only the P-9, but also other development vehicles with varying mass and levels of propellant. The next section describes the development of the engine meeting these requirements.

Table 1. Baseline NLV stage characteristics

	1st Stage	2nd Stage
Dry mass	171 kg (378 lb)	30 kg (67 lb)
Stage inert mass fraction	0.131	0.137
Chamber pressure	2 MPa (300 psi)	1 MPa (150 psi)
Sea-Level Thrust	20,000 N (4,500 lbf)	N/A
Sea-Level ISP	212 s	N/A
Vacuum Thrust	29,600 N (6,660 lbf)	1,900 N (430 lbf)
Vacuum ISP	314 s	347 s
Separation/ burnout time (from lift off)	117 s	455 s
Separation/ burnout altitude	54 km	250 km, orbital

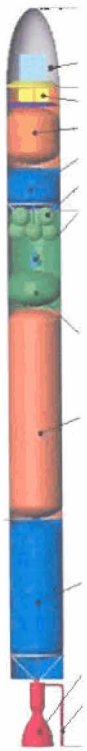

Figure 1. Baseline NLV

Table 2. RLV and NLV performance characterization compairson

Vehicle	P-7D	P-9A/B	NLV 1st stage
T/W @ L.O.	3.75	4.2	1.33
Thrust @ L.O.	1030 lbf (4600 N)	3500 lbf (15,600 N)	4500 lbf (20,000 N)
Fuel (/ LOX)	Ethanol	Ethanol	Propylene
Dry mass	228 lb (104 kg)	507 lb (230 kg)	378 lb (171 kg)
Propellant load (Mass and % of tanks)	51 lb (23 kg)	214 lb (97 kg) 13%	2500 lb (1,137 kg)
Burn time	9 s	13 s	116 s
Peak altitude	3.5 kft (1.06 km)	18.9 kft (5.8 km)	177kft (54 km) @ burnout
Other	Small tanks Blow-down	Full size tanks Blow-down	Carries 530 lbm loaded 2nd stage

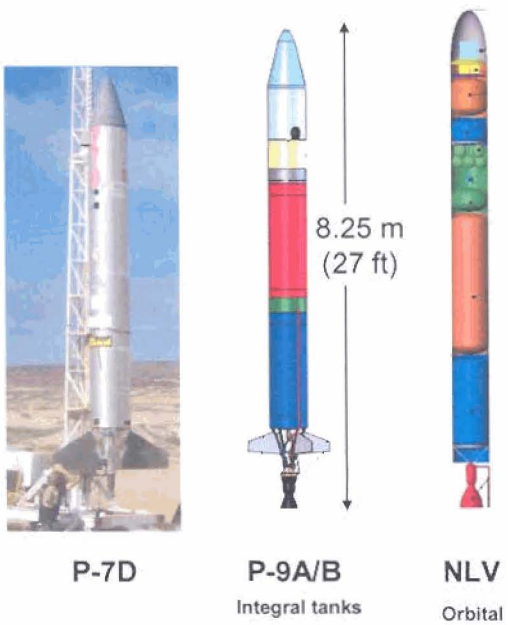

Figure 2. Comparison between suborbital RNLV's and the orbit capable NLV (images to scale)

Table 3 Nominal engine performance and range of operations

	RLV	NLV
Propellants	LOX/Ethanol	LOX/Propylene
Nominal thrust	4,500 lbf (20kN)	4500 lbf (20kN)
Thrust range	2550 - 5095 lbf (11,300 – 22,640 N)	2550 - 5095 lbf (11,300 – 22,640 N)
O/F	1.4 ± 0.1	2.4 ± 0.1
Nominal Chamber pressure, Pc	265 psia (1.8 MPa)	300 psia (2 MPa)
Pc range	150-300 psia (1.0 to 2.0 MPa)	150-300 psia (1.0 to 2.0 MPa)
ε	6	12
Burn duration	10 s to 100 s	120s

II. Engine Description

A. Overview

The engine (Figure 3) is comprised of three major subassemblies; the injector, igniter, and the combustion chamber/nozzle. Table 4 shows the target engine characteristics.

During the preliminary design of the engine, two engine configurations were traded, one with a flat head injector and the other with a pintle injector (Figure 4). The flat head injector provides increased combustion efficiency but is more difficult to machine. The pintle injector presents lower combustion efficiency and greater difficulty in controlling the O/F distribution in the chamber. The decision was made to adopt the flat head injector due to its increased performance

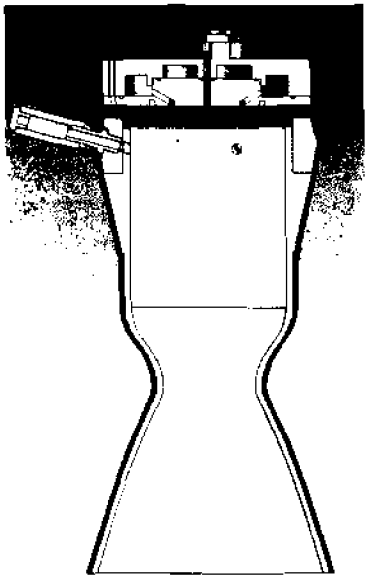

Figure 3. Engine configuration

Table 4. Nominal engine characteristics

Thrust	4,500 lbf
ε	6
Pc	265 psi
O/F	1.4
$\eta c^*, \lambda$	0.9
$ISP_{S.L.}$	190 s
ISP_{VAC}	237 s

B. Injector

The injector (Figure 5) has three different sets of orifices (Figure 6). The inner set has unlike doublets, the middle set unlike split triplets, and the outer ring is used for film cooling, (15% of the fuel flow). One of the key design features of the injector is that it can be removed from the chamber without completely dissembling the injector; this greatly reduces engine assembly time and eases integration. One of these features is the central bolt that is used to keep the engine o-rings compressed while the injector is installed to the engine chamber. This bolt when torqued to 12 ft-lb generates approximately 4000 lbf of preload on the bolt to prevent the bottom plate from bowing during engine operations. Once the injector has been manufactured, impingement is verified with a water-flow test (Figure 7) and orifices are adjusted to obtain the desired oxidizer-to-fuel ratio (O/F), and determine the discharge coefficient of the injector and its pressure drop.

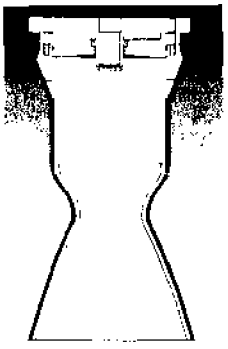

Figure 4. Pintle injector design alternative

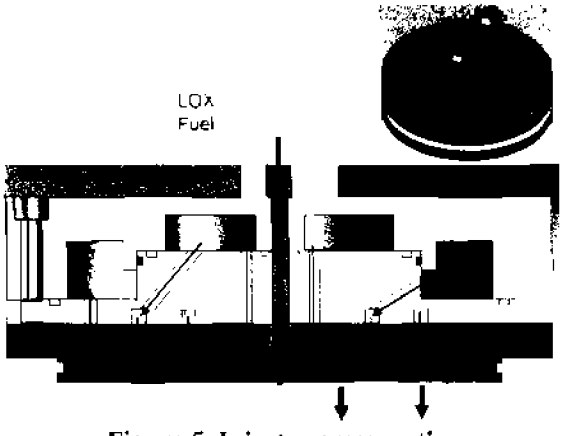

Figure 5. Injector cross section

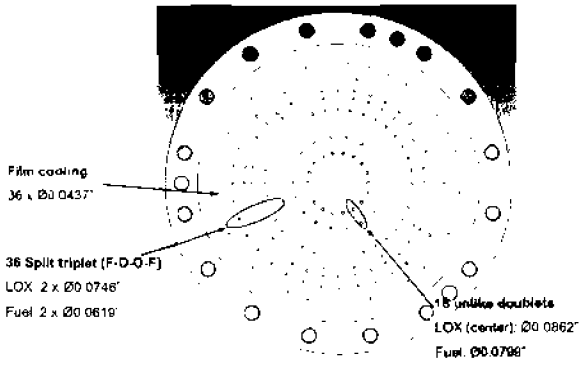

Figure 6. Injector orifice pattern

Figure 7. Injector water flow testing (fuel side shown)

C. Chamber/Nozzle

The combustion chamber and nozzle assembly is an ablative with the first development articles made with a silica tape and high temperature epoxy resin. For longer duration burns, silica/phenolic is used. The ablative liner is over-wrapped with carbon fiber epoxy to add extra strength to the chamber and nozzle.

The combustion chamber is cylindrical in shape, is 7.08 inches in diameter and 12 inches long with a 3 degree draft to allow for easy release from the mold used to lay-up the ablative chamber (Figure 8). The throat diameter is 4.22 inches and the exit diameter is 10.33 inches which results in an expansion ratio of 6.

D. Igniter

Ignition was first accomplished by using six small pyrotechnic lances which were inserted through the nozzle. This represented a scaling up from the ignition configuration employed on smaller engines. These were later replaced with a more reliable system which consisted of three class D solid propellant motors firing radially inward from ports mounted to the side of the chamber flange. Each port contains both the propellant motor as well as a thermocouple to monitor the igniter temperature as seen in Figure 9. The three igniter ports are angled 15 degrees away from the injector, so as to not scorch the face of the injector. This configuration also facilitates rapid removal and replacement for quick turnaround between tests. The algorithm that lights the igniters is outlined below.

Figure 8. Engine chamber mold

Figure 9. Igniter port with thermocouple

III. Initial Tests

The engine has undergone several tests which consist of 6 horizontal static fire tests, 4 vertical static fire tests and, one flight test. Tests were instrumented with a variety of pressure, temperature and load cell sensors. The data collected is used to compute the propulsion system and engine performance using a student-developed post processor implemented in LabVIEW. The processor takes in the raw data recorded

during the test as well as characteristics of the engine and calculates the various performance parameters, such as mass flow rates, combustion and nozzle efficiencies, oxidizer to fuel ratio, and ISP.

A. *Ignition Tests*

The engine was first tested on a horizontal test stand (Figure 10) in order to validate the ignition algorithm, verify the engine basic integrity at startup, and characterize the engine performance under nominal conditions as well as over a broader range of operating conditions. Once the tanks have been pressurized the ignition sequence begins at T-10. At T-3 the command is sent to turn on the igniters. The algorithm monitors igniter temperature and when it determines that at least two out of three igniters have lit and are increasing in temperature the command is sent automatically to open the main valves at T-0. At the end of the predetermined burn time the command is sent to close the main valves, and when the chamber pressure drops below 100 psi, the injector and chamber are purged with GN2. Figure 11 illustrates typical igniter temperature behavior during igniter start-up. Due to small setup variations, it is common that two of the three igniters light simultaneously while the third lags slightly behind. The system behavior during start-up is shown in Figure 12 which depicts the variation of pressures in the propellant tanks, in the feedlines right upstream of the injector (denoted "injector") and in the chamber. In this configuration, the LOX and fuel valve had separate pneumatic actuation systems. The LOX valve starts opening at 75 ms while the fuel valve opens about 160 ms after the command is issued leading to a smooth ramp up of the combustion chamber pressure. The oscillation visible in the fuel injector pressure is from the incompressibility of ethanol.

Figure 10. First horizontal static fire test

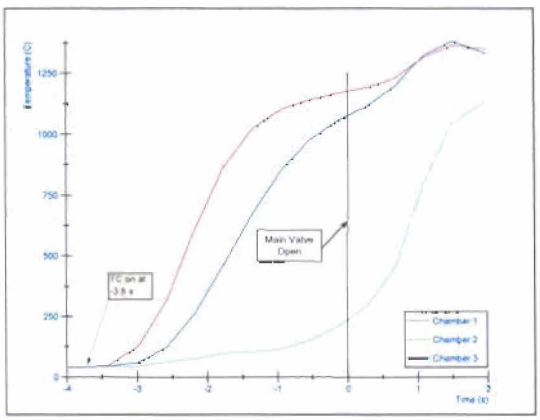

Figure 11. Igniter thermocouples from SFT-4500-02A

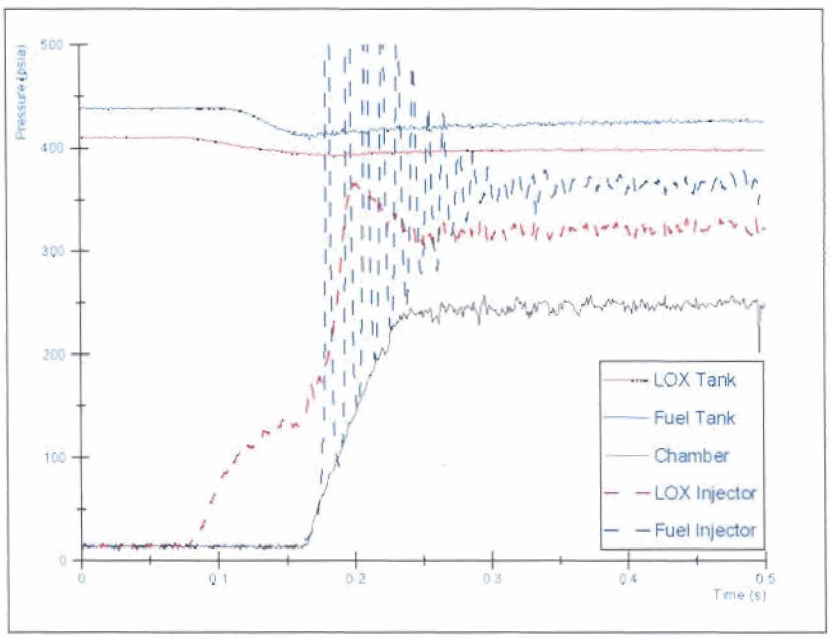

Figure 12. Engine ignition from SFT-4500-02D

Six tests were conducted in this configuration, producing a wide array of thrusts levels ranging from 2500 to 5074 lbf as illustrated in Table 5, due to varying startup conditions. In order to characterize the engine performance for various vehicle pressurization configurations, tests were conducted for two different operating conditions, regulated-helium mode and simulated blow-down mode. During a simulated blow-down test (run 02A in Figure 13), the engine experienced chugging starting at 140 psia, a low frequency form of combustion instability in which the pressure drop across the injector is low enough to couple combustion dynamics with the feed system. The pressure and force profiles of the engine operating under constant feed pressure conditions and blow-down are shown in Figure 13 and Figure 14, respectively.

Table 5. Horizontal static fire test engine operations

	SFT-4500-01A	SFT-4500-02A	SFT-4500-02B	SFT-4500-02C	SFT-4500-02D
Burn time	4.5 s	6 s	3 s	No Data Collected	4.5 s
Note	Regulated	Blow-down	Blow-down		Regulated
Chamber Pressure	258 psia	max 196 psia min 108 psia	max 183 psia min 138 psia		270 psia
Engine Thrust	4687 lbf	max 3170 lbf min 1638 lbf	max 3125 lbf min 2467 lbf		max 5074 lbf

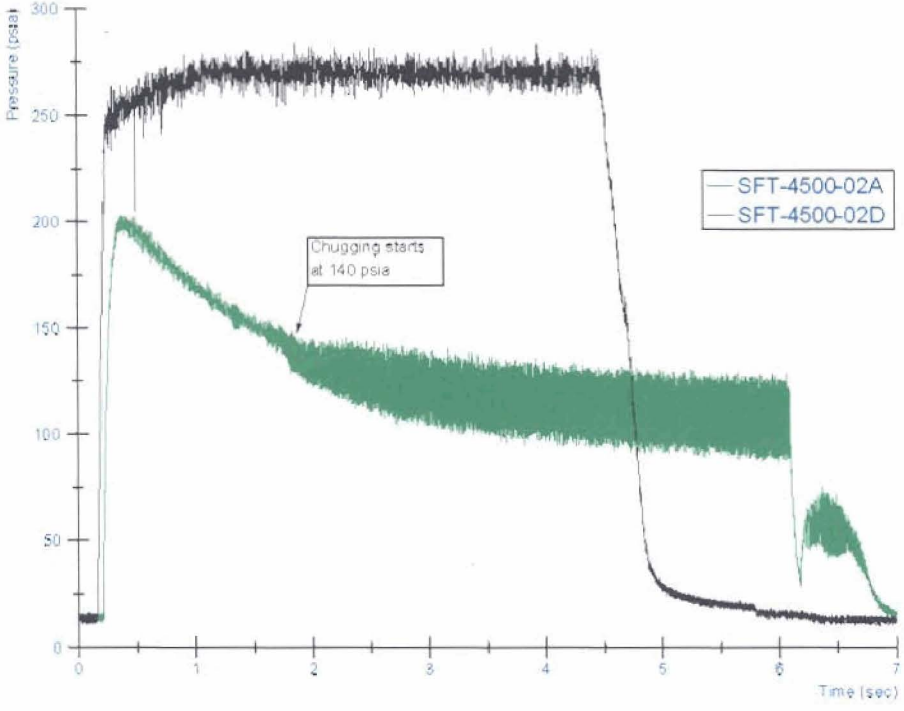

Figure 13. Chamber pressure comparison between simulated blow-down run (green, 02A) and regulated pressure run (black, 02D)

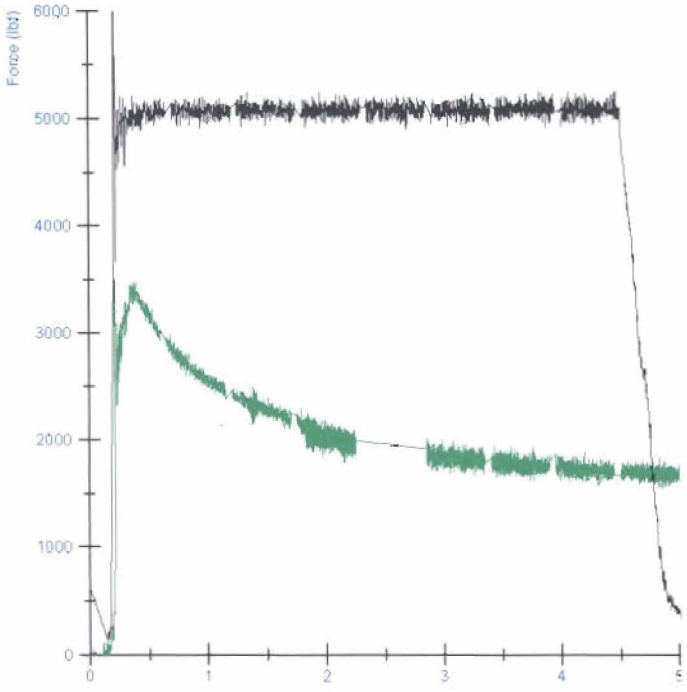

Figure 14. Force comparison corresponding to

Figure 15. First vertical static fire test

B. Engine in Vehicle Propulsion System

The next set of tests were conducted on a vertical test stand in which the engine was integrated to a prototype launch vehicle, the Prospector-8A (P-8A, Figure 15) in order to characterize the engine into a vehicle propulsion system, in preparation for follow-on flight tests. In order to limit lift-off acceleration to around 7 g's, the engine operating pressure was reduced to obtain a thrust between 3,000 and 3,500 lbf.

Four tests were conducted in the P-8A configuration, most notably using a regulated helium pressurization system. The GHe is stored in a 1623 cu inch tank DOT-rated to 3295 psi. Both LOX and fuel tank clusters have a capacity of 12.5 gal.

The testing verified that the vehicle propulsion system worked with the engine and demonstrated relatively consistent performance across all tests, as indicated in Table 6. Figure 16 depicts a typical engine startup, here from VSFT-4500-02B and, by comparing it with Figure 12, shows that the ignition characteristics for both horizontal and vertical tests are similar despite using two new main propellant valves operating simultaneously with a single actuator. Two short duration burns were conducted, the first to verify ignition with the new propulsion system and the second w to verify engine integrity after an injector design modifications because of an earlier injector failure. An eight second burn was then conducted, corresponding to the flight conditions expected during the planned P-8A flight test. Figure 17 depicts the steady state portion of the burn used for the performance calculations. A longer burn could have been conducted but the test duration was limited by the flame deflector life.

Figure 18 depicts a comparison between the predicted pressure profile of the vehicle helium (GHe) tank and measured data from VSFT-4500-02B. From the measured injector pressure drop during the static fire test and the discharge coefficients determined from the earlier water-flow test, engine flow rates and O/F can be estimated. These flow rates are shown in Figure 19 for both propellants, and the engine, along with the engine O/F. The O/F was measured at 1.28, less than the predicted O/F of 1.36 because the water flow test did not replicate the longer LOX feedlines of the P-8A vehicle (the LOX tanks are located in the section of the vehicle covered in aluminized insulation in Figure 15). Figure 20 and Figure 21 show typical engine performance. Even with the limited number of orifices used in the early low cost prototype, the c*

efficiency, η_{c^*}, exceeds 90%. The nozzle efficiency obtained during this test is lower than measured in previous tests (above 95%) because of severe de-lamination of the ablative liner in the nozzle.

Table 6. Vertical static fire test engine operations

	VSFT-4500-01A	VSFT-4500-02A	VSFT-4500-02B
Burn time	1.8 s	3 s	8 s
Notes	Regulated	Regulated	Regulated
Chamber Pressure	223 psia	189 psia	208 psia
Engine Thrust	3261 lbf	2950 lbf	3508 lbf
c* efficiency, η_{c^*}	N/A	74%	88%
Nozzle efficiency, λ	N/A	87%	90%

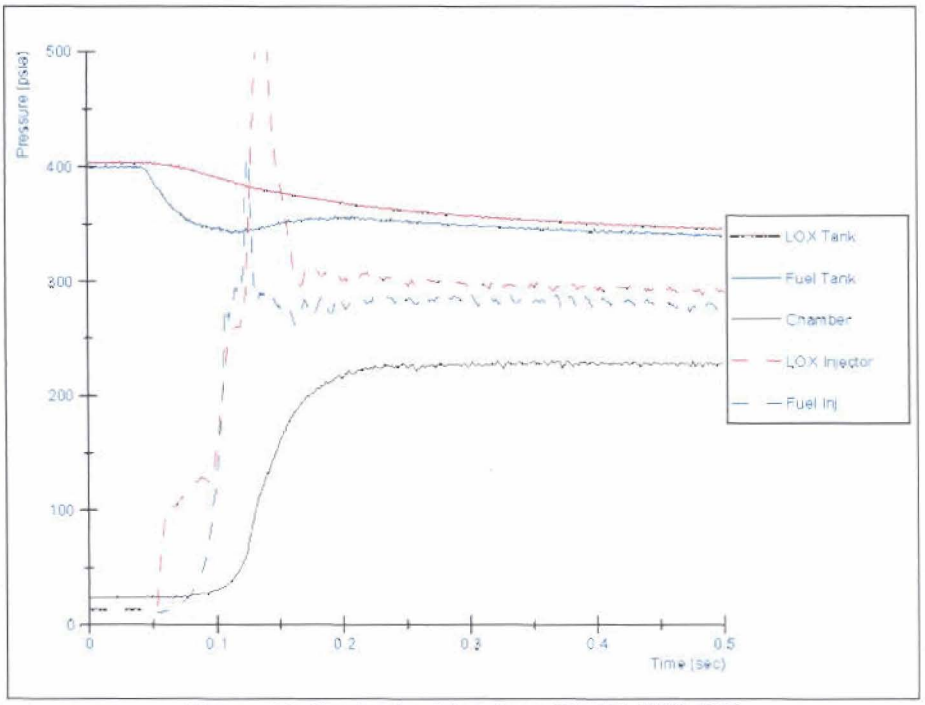

Figure 16. Engine ignition from VSFT-4500-02B

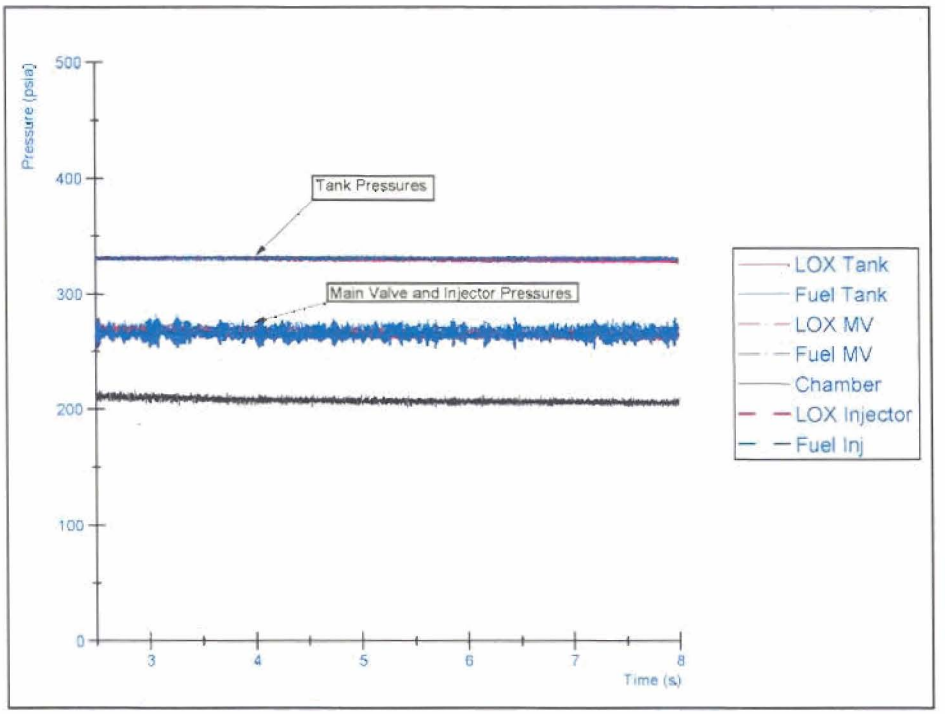

Figure 17. Pressure variations during VSFT-4500-02B – steady-state portion of the burn, approx. 2.5 s to 8 s.

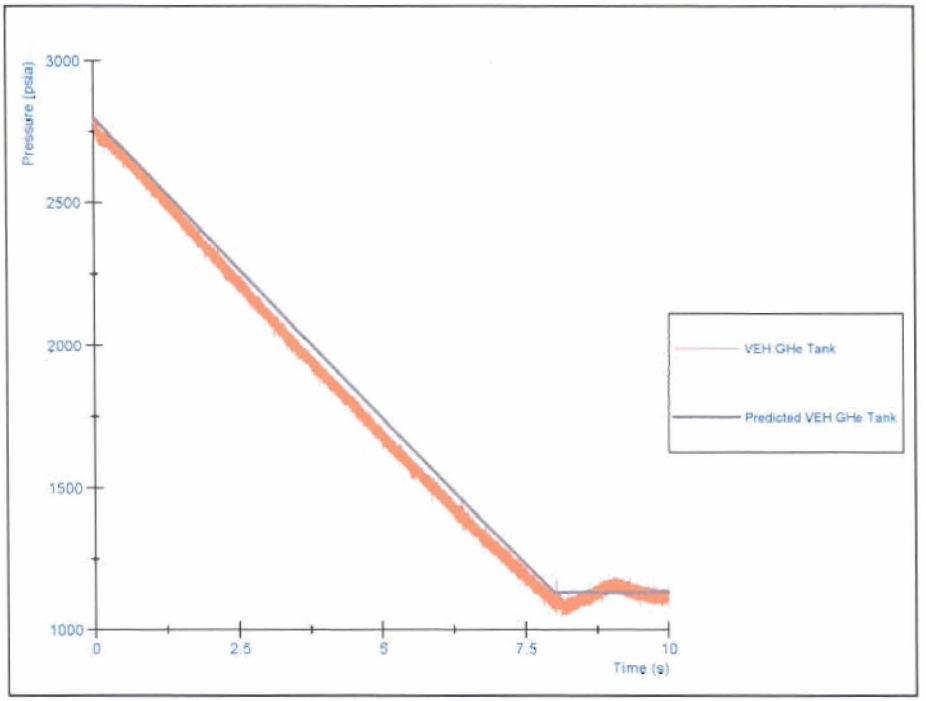

Figure 18. Predicted vehicle GHe tank pressure versus measured GHe tank pressure

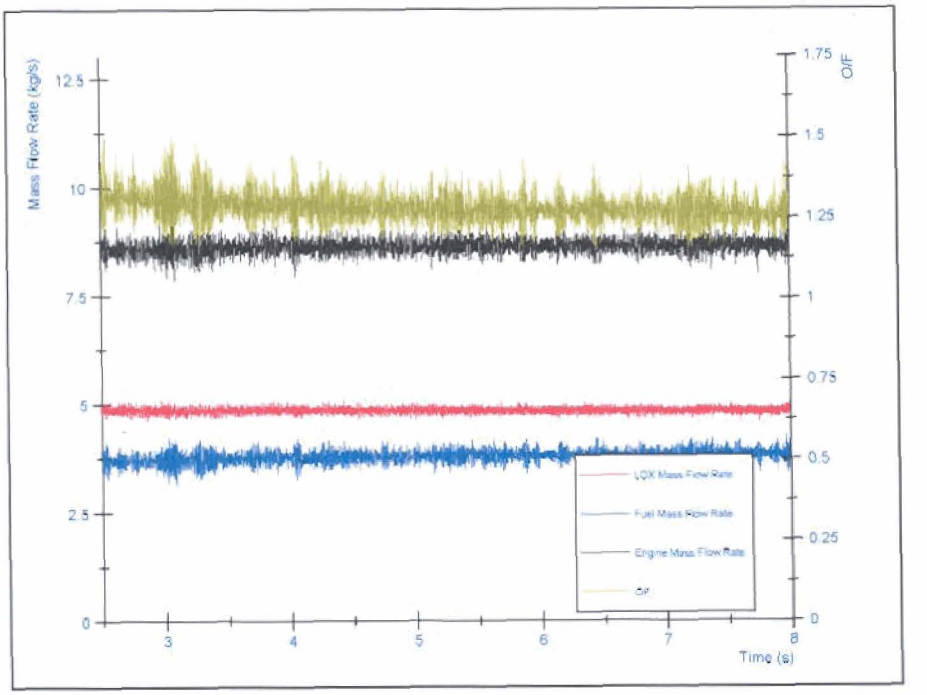

Figure 19. Mass flow rates and O/F for VSFT-4500-02B

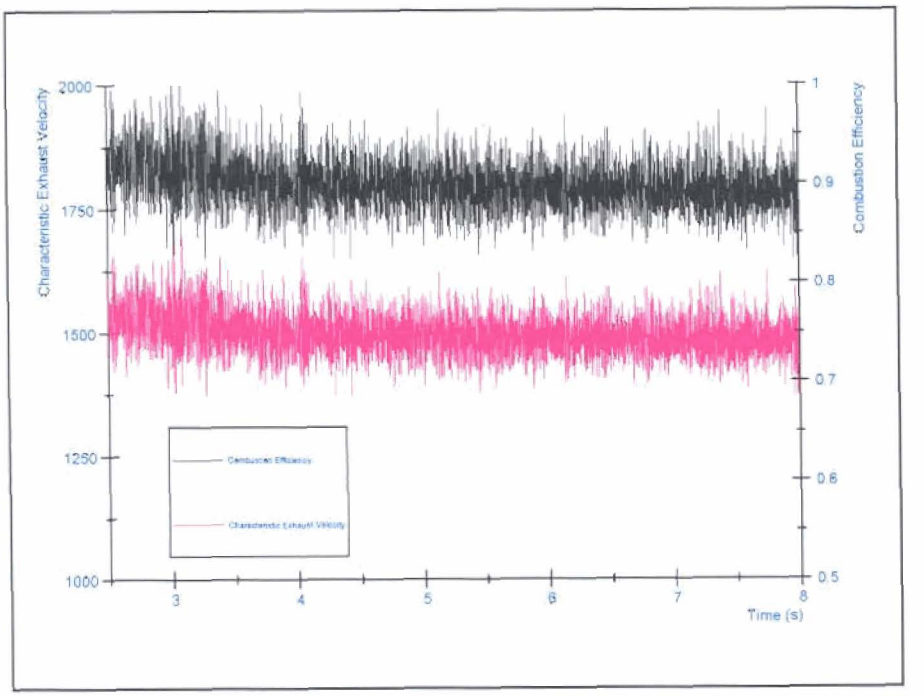

Figure 20. Characteristic velocity, c*, and c* efficiency, η_{c^*}, measured from VSFT-4500-02B

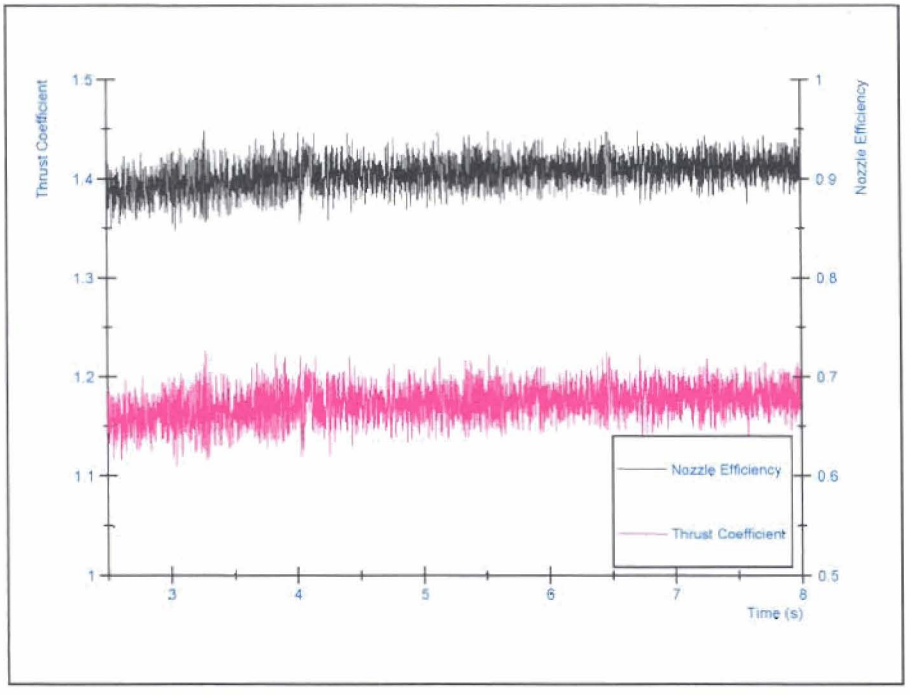

Figure 21. Thrust coefficient, C_F, and nozzle efficiency, λ, measured in VSFT-4500-02B

C. Flight Test Demonstration

With the completion of the static tests, a flight test was conducted in Sept. 2007 (Figure 22). In order to limit the vehicle apogee and downrange landing, the P-8A was only half loaded with propellants. In those conditions, it burns out near supersonic conditions and its estimated maximum altitude was approximately 15,000 ft. Its expected trajectory is shown in Figure 23 and key mission points are described in Table 7. Again, due to the relatively light weight of P-8A, tank pressures were set such that the chamber pressure was reduced from the engine baseline of 265 psia to 220 psia, which in turn reduced the engine thrust to approximately 3500 lbf. Even with this reduction in thrust, P-8A still had a net 7 g liftoff. The predicted Mach number variation during the mission is shown in Figure 24 and indicates that the rocket would reach sonic conditions at engine burnout.

Almost 4 seconds after liftoff and nearing 800 ft/s, however, fin flutter occurred which led to the destruction of the fins, causing the rocket to become unstable while powered. The parachute partially deployed and the vehicle was recovered, with many components such as the engine usable for future flights. Post-flight flutter analysis was conducted and confirmed that the thin carbon-fiber fins as built were prone to flutter[11]. Future vehicles, such as the P-9, will feature stiffer fins much less sensitive to twisting so as to avoid flutter throughout the flight regime.

(a)  (b) 

Figure 22. (a) CALVEIN team before flight and (b) P-8A in flight

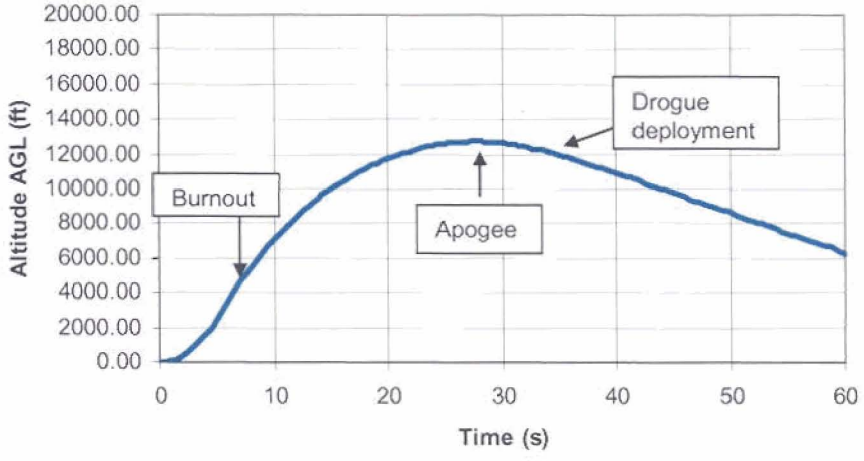

Figure 23. Predicted P-8A trajectory

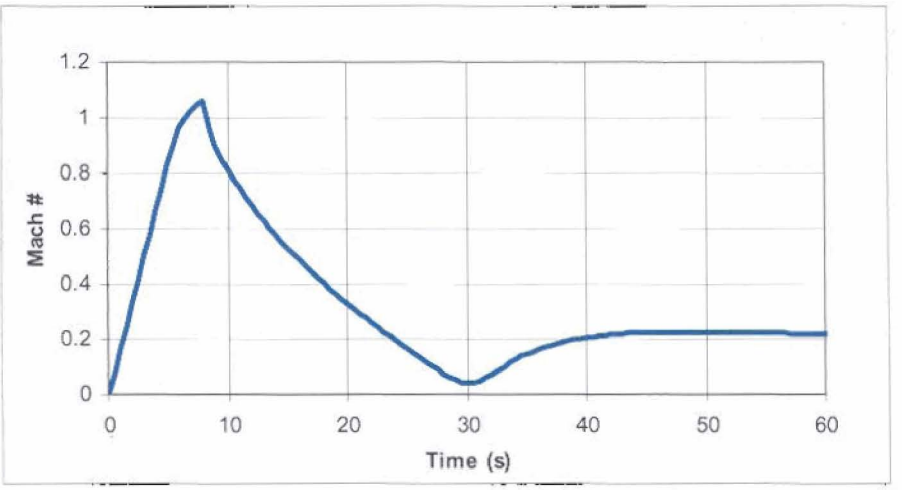

Figure 24. Predicted Mach # versus time

Table 7. Summary of trajectory events

Trajectory events	Lift-off	Burn out	Apogee	Drogue deployt.	Parachute deployt	Touch-down
Time (s)	0	6.27	28	32	86	108
Altitude AGL (ft)	0	3816	12739	12484	699	0
Pc (psia)	218	192	0	0	0	0
Mach #	0.00	1.00	0.04	0.12	0.19	0.03
Thrust (lbf)	3498	3097	0	0	0	0
Horizontal speed (ft/s)	0	77	38	36	-9	-9
Vertical speed (ft/s)	0	1087	0	-127	-206	-31
Range (ft)	0	231	1244	1392	1296	1100

Conclusion & future steps

Initial testing discussed in the paper shows that the engine design meets nominal performance requirements and is able to operate in a wide range of conditions to successfully power a wide family of low-cost prototype launch vehicles. The next engine development steps involve longer duration burns in order to evaluate silica-phenolic ablative materials instead of the silica-epoxy used for the short duration burn tests shown here, as well as determining the behavior of the injector during longer burns. Follow-on steps will also be taken to improve performance, such as by increasing the number of orifices, modifying the passages in order to reduce engine weight, and eventually transitioning from ethanol to propylene.

Acknowledgments

The engine development was funded by a Phase II SBIR, contract no. AFFTC/PKTA PO FA9300-06-C-0009 between AFRL and GSC with CSULB participating as primary subcontractor to GSC. The authors would also like to recognize the numerous CSULB/GSC team members who assisted in the development of the engine and associated systems.

References

[1] J. Garvey, E. Besnard, G. Elson and K. Carter, "The Incremental Development of a Cost-Effective Small Launch Vehicle for Nanosat Payloads," AIAA Paper No. 03-6390, presented at Space 2003, Long Beach, CA, Sept. 2003.

[2] J. Garvey and E. Besnard, "A Status Report on the Development of a Nanosat Launch Vehicle and Associated Launch Vehicle Technologies," AIAA Paper No. 04-7003, presented at the 2nd Responsive Space Conference, Los Angeles, CA, April 2004.

[3] J. Garvey and E. Besnard, "Development of a Dedicated Launch System for Nanosat-Class Payloads," Paper No. SSC04-X-3, 18th AIAA/USU Conference on Small Satellites, Logan, UT, Aug. 2004.

[4] J. Garvey and E. Besnard, "Progress Towards the Development of a Dedicated Launch System for Nanosat Payloads," AIAA Paper No. 04-6003, presented at Space 2004, San Diego, CA, Sept. 2004.

[5] J. Garvey and E. Besnard, "LOX-Propylene Propulsion testing for a Nanosat Launch Vehicle," AIAA Paper No. 05-4294, presented at the Joint Propulsion Conference, Tucson, AZ, July 2005

[6] J. McCall and E. Besnard, "Validating C/SiC Composites for Liquid Bipropellant Thrusters: Analysis of a 500 lbf Thrust LOX/propylene Rocket Engine," presented at the 53rd Joint Army-Navy-NASA-Air Force (JANNAF) Propulsion Meeting, Monterey, CA, Dec. 2005.

[7] J. Garvey and E. Besnard, "Ongoing Nanosat Launch Vehicle Development for Providing Regular and Predictable Access to Space for Small Spacecraft," Paper No. SSC05-X-2, 19th AIAA/USU Conference on Small Satellites, Logan, UT, Aug. 2005.

[8] J. Garvey and E. Besnard, "Initial Results of Nanosat Launch Vehicle Developmental Flight Testing," AIAA Paper 2005-6641, presented at the Space 2005 conference, Long Beach, CA, Aug. 2005.

[9] J. Garvey and E. Besnard, "RLV Flight Operations Demonstration with a Prototype Nanosat Launch Vehicle," AIAA Paper 2006-4787, presented at the 42nd Joint Propulsion Conference, Sacramento, CA, July 2006.

[10] J. Garvey and E. Besnard, "Initial Results from the Demonstration and Analysis of Reusable Nanosat Launch Vehicle Operations," presented at the 54th Joint Army-Navy-NASA-Air Force (JANNAF) Propulsion Meeting, Denver, CO, May 2007.

[11] J. Garvey, E Besnard and N. Sedano, "Rapid Turn-Around Flight Testing of a Next-Generation Prototype RLV," AIAA Paper No. 2008-5209, July 2008.